

# Isolation of rafts from mouse brain tissue by a detergent-free method

Dixie-Ann Persaud-Sawin,<sup>1</sup> Samantha Lightcap, and G. Jean Harry

Laboratory of Molecular Toxicology/Neurotoxicology Group, National Institute of Environmental Health Sciences, RTP, NC 27709

**Abstract** Membrane rafts are rich in cholesterol and sphingolipids and have specific proteins associated with them. Due to their small size, their identification and isolation have proved to be problematic. Their insolubility in non-ionic detergents, such as Triton-X 100, at 4°C has been the most common means of isolation. However, detergent presence can produce artifacts or interfere with ganglioside distribution. The direction is therefore toward the use of detergent-free protocols. We report an optimized method of raft isolation from lipid-rich brain tissue using a detergent-free method. We compared this to Triton-X 100-based isolation along sucrose or Optiprep™ gradients using the following endpoints: low protein content, high cholesterol content, presence of Flotillin 1 (Flot1), and absence of transferrin receptor (TfR) proteins. These criteria were met in raft fractions isolated in a detergent-free buffer along a sucrose gradient of 5%/35%/42.5%. The use of optiprep gave less consistent results with respect to protein distribution. We demonstrate that clean raft fractions with minimal myelin contamination can be reproducibly obtained in the top three low-density fractions along a sucrose step gradient.—Persaud-Sawin, D-A., S. Lightcap, and G. J. Harry. **Isolation of rafts from mouse brain tissue by a detergent-free method.** *J. Lipid Res.* 2009. 50: 759–767.

**Supplementary key words** lipid-rich compartments • Flotillin 1 • liquid-disordered phase • membrane

Eukaryotic cell membranes consist of liquid-ordered states surrounded by liquid-disordered phases. This arrangement allows for the existence of small, organized membrane microdomains called rafts (1–5) that orchestrate and regulate a number of signaling processes (6–13). In order to elucidate mechanisms involved in these processes, it is crucial to understand raft biology. A major obstacle, however, has been that their isolation and characterization have been problematic. Lipid rafts are typically obtained by flotation through continuous or discontinuous

gradients. Their insolubility in nonionic detergents, such as Triton-X 100, Brij 96, Lubrol series, and Nonidet P40, at 4°C has enabled the isolation of raft-like structures termed detergent resistant membranes (DRMs) that have low buoyant densities and the ability to float on sucrose gradients. DRMs, like rafts, float away from detergent-soluble proteins and cytoskeletal proteins. The introduction of Iodixanol (Optiprep™) provided researchers with an alternative to sucrose as a density gradient medium that is iso-osmotic up to a density of 1.32 g/ml (14).

Many studies have shown that some nonionic detergents fail to release DRMs at physiologically relevant temperatures (15, 16). This led to the main controversy in the raft field: that DRMs, and therefore rafts, may be artifacts of preparation (17). However, the data supporting the existence of rafts are steadily growing. For instance, it has recently been shown that DRMs can be isolated at 37°C with nonionic detergents (18). Despite this there are caveats. Different detergents can yield varying subsets of DRMs, each with unique properties (19–24); introduce artifacts not representative of membranes (25); cause abnormal redistribution of gangliosides; or alter raft properties (20). The presence of detergents can also interfere with organelle and raft integrity (26), and may even produce anomalous or false-positive results, such as the unnatural oligomerization of amyloid-β (27). Therefore, the general consensus is toward the use of detergent-free protocols. Such methods would provide the investigator not only with the option to use the isolated fractions for analyses where detergent presence would be detrimental, such as in proteomic or lipid analyses and screening (21), but would also allow additional characterization of rafts.

Most reports document the isolation of rafts from cultured cells (1, 15, 28, 29). Although studying rafts in cell lines allows the investigator to examine the raft contribution from a single cell type, using tissue enables the exami-

*This research was supported by the Intramural Research Program of the National Institutes of Health, National Institute of Environmental Health Sciences under project #1Z01ES101623-05.*

*Manuscript received 18 July 2008 and in revised form 3 December 2008.*

*Published, JLR Papers in Press, December 6, 2008.  
DOI 10.1194/jlr.D800037-JLR200*

Abbreviations: DRM, detergent resistant membrane; Flot1, flotillin 1; GRASP65, Golgi reassembly and stacking protein 65; MBP, myelin basic protein; PMSF, phenylmethanesulphonyl fluoride; PND, postnatal day; TfR, transferrin receptor.

<sup>1</sup>To whom correspondence should be addressed.  
e-mail: sawind@niehs.nih.gov

nation of raft dynamics and proteolipid interaction within the organ system as a whole. The dynamic functions of lipid rafts have been reflected in the recent implication that they may be involved in the pathogenesis of many neurodegenerative conditions (30–34). These studies, as well as raft interactions for signal transduction, membrane trafficking, and endocytosis, emphasize the value of examining whole tissue in the hope of determining regional brain, genetic, or age-specific effects. The brain represents one target tissue for which the role of membrane rafts in various disease conditions has more recently become of interest (10, 31, 33, 35–37), and is therefore, the focus of this protocol. The majority of the work examining the role of rafts in the nervous system has relied on either primary cell cultures or isolated cellular preparations, such as from synaptosomes (38) and microvesicles (39). This is due substantially to the large amount of lipid present in brain white matter in the form of myelin, which increases with age. For instance, at 6 months of age, 60 mg of myelin can be isolated from the rat brain, compared with only 4 mg at postnatal day (PND) 15 (40). Thus, there should be a lower probability of myelin contamination of rafts isolated from PND 21 animals than from adult or older animals. By PND 21, myelin basic protein (MBP), a major myelin protein, has already been laid down in its mature form and is associated with raft fractions (41). MBP is involved in the maintenance of myelin and axonal integrity and may be associated with delayed-onset neurodegeneration (42). It has also been used as an indicator of raft structural integrity (43). Additionally, there is an age-dependent accumulation of ubiquitinated 2',3'-cyclic nucleotide 3'-phosphodiesterase (CNP) in isolated myelin rafts (34), which may alter their steady-state. We therefore chose to use PND21 mice as our model in this study, in lieu of adult mice.

Regarding tissue protocols, raft-structures have been primarily isolated via detergent methods (19, 23, 44). Although some use with nondetergent methods have been employed for brain cellular structures, these studies have used purified preparations (38, 39, 45) and are not truly representative of brain tissue. Additionally, previously used protocols have multiple, long centrifugation and sonication steps that can result in the over-abundance of proteins not normally present within rafts and produce low yields. Another problem is the use of postnuclear supernatant (PNS) sources where both the source type and gradient can contain some form of detergent. MacDonald and Pike (48) recently adapted detergent-free protocols from Song et al. (46) and Smart et al. (47) into a time-efficient method of raft isolation from cell line-derived PNS sources. Their protocol involves isolation of purified rafts by shearing cells in an isotonic buffer with cations, followed by separation along a 0% to 20% continuous OptiPrep™ gradient. This procedure has recently been used to isolate rafts from purified preparations of rat cerebral microvessels (39). Other detergent-free methods have used sodium carbonate and OptiPrep™; magnetic bead; or silica-based isolations using raft/caveolar proteins as markers or the use of cationic buffers, which may stabilize raft-associated proteins (47–50).

While these methods are useful for isolating rafts from isolated cells or cell structures, they have not been applied to whole tissue. Here, we employ the original MacDonald and Pike protocol (48) as a starting point, and our optimization of this method for use on unprocessed brain tissue in the context of raft integrity.

## EXPERIMENTAL PROCEDURES

### Materials

Calcium chloride, magnesium chloride, sucrose, sodium fluoride, sodium orthovanadate, phenylmethanesulphonyl fluoride (PMSF), and protein inhibitor cocktail were obtained from Sigma-Aldrich (St. Louis, MO). SW60 ultracentrifuge tubes (#328874) were obtained from Beckman (Palo Alto, CA). BCA protein assay (#23227) and SuperSignal West Pico Chemiluminescent substrate were obtained from Pierce (Rockford, IL). Flotillin1 antibody (cat# 610821, BD Biosciences, Franklin Lakes, NJ), transferrin receptor antibody (TfR; cat# 13-6800, Zymed, San Francisco, CA), MBP antibody (cat# NBA-116, Assay Designs, Ann Arbor, MI), and Golgi reassembly and stacking protein 65 (GRASP65) antibody (cat# ab30315, Abcam, Cambridge, MA) were used for Western blots. Invitrogen (Carlsbad, CA) Western Breeze Chemiluminescent kits were used for Western blot protein detection. Optiprep™ was obtained from Axis-Shield (Norton, MA). The Cholesterol Assay Kit (#10007640) was obtained from Cayman Chemicals (Ann Arbor, MI). DMEM media, horse serum and FBS (entodoxin level < 0.1 EU/ml) were obtained from Invitrogen.

### Animals

PND 21 and adult (3 months old) C57BL/6 mice (Charles River Labs, Raleigh, NC) were anesthetized with CO<sub>2</sub>, decapitated, and brains excised. Cortical tissue from both hemispheres was dissected to obtain the cortex and underlying corpus callosum. The brainstem was also removed. One hundred milligram samples were immediately frozen on dry ice in microfuge tubes and stored at –80°C. Samples could be stored for a maximum of 1 year. All procedures were conducted according to an NIEHS Animal and Care Use Committee approved protocol.

### Isolation procedures

*Detergent-free method.* TISSUE HOMOGENIZATION. Frozen brain tissue samples were thawed on ice and homogenized in 500  $\mu$ l of detergent-free lysis buffer [1 $\times$  TBS (pH 8), 1% proteinase inhibitor cocktail, 1 mM PMSF, 5 mM NaF, 1 mM Na Orthovanadate] with the addition of 1 mM CaCl<sub>2</sub> and 1 mM MgCl<sub>2</sub> to render rafts more stable (23). The homogenate was sheared through a 23-gauge needle with 20 complete passes then centrifuged at 1,000 *g* for 10 min at 4°C and the PNS removed and maintained on ice. The process was repeated on the pellet. The final pellet was discarded unless required for comparison between cortex and brainstem tissues. The supernatants from both shearing steps were pooled and stored at –80°C for use later or immediately subjected to density gradient ultracentrifugation along sucrose or OptiPrep™ step density gradients.

SUCROSE STEP DENSITY GRADIENT. All steps were performed on ice and all reagents precooled to  $\leq$ 4°C. Two hundred twenty-five microliters of the pooled supernatant was placed in pre-cooled SW60 ultracentrifuge tubes on ice and 225  $\mu$ l of 85% sucrose/TBS mixed with gentle pipeting to prevent the

formation of bubbles. To this, 3.0 mls of 35% sucrose/TBS was overlaid, followed by 675  $\mu$ l 5% sucrose/TBS. This 5%/35%/42.5% gradient was compared with a 5%/20%/30% sucrose gradient. The tubes were centrifuged at 38,500 rpm (200,000  $g$ ) for 18 h at 4°C and compared with a 4 h spin time. Acceleration and deceleration rates were set to zero. After centrifugation, the mixture was clear except for a distinct, cloudy band at the interface between the 5% and 35% sucrose. Fifteen sequential fractions of 260  $\mu$ l each were gently removed from the top of the tube and individually aliquoted. High-density fractions 14 and 15 were pooled as they are not normally considered as raft fractions (1, 10, 28). The fractions were stored at  $-80^{\circ}\text{C}$  for a maximum of 6 months.

**OPTIPREP™ STEP DENSITY GRADIENT.** To SW60 ultracentrifuge tubes, 225  $\mu$ l of the pooled supernatant was added and mixed with 225  $\mu$ l of 50% Optiprep™. To this, 3.0 mls of 20% Optiprep™ was overlaid, followed by 675  $\mu$ l 10% Optiprep™. The tubes were centrifuged at 38,500 rpm (200,000  $g$ ) for 18 h at 4°C. Acceleration and deceleration rates were set to zero. Fifteen fractions of 260  $\mu$ l each were gently removed from the top of the tube and individually aliquoted. High-density fractions 14 and 15 were pooled. The fractions were stored at  $-80^{\circ}\text{C}$  for up to 6 months.

*Detergent method.* While recent data identified confounding effects with detergent use, a significant amount of previous data on membrane rafts is based on the use of detergent-based isolation. We therefore compared isolation of rafts to the Triton-X 100 detergent method of preparing DRMs.

All steps of the procedure were carried out with the tissue maintained on ice. Tissue was thawed on ice and homogenized in 500  $\mu$ l of lysis buffer with detergent [1 $\times$  TBS (pH 8), 1% Triton-X 100, 1% proteinase inhibitor cocktail, 1 mM PMSF, 5 mM NaF, 1 mM Na orthovanadate] and incubated on ice for 30 min. The homogenate was centrifuged at 1,000  $g$  for 10 min at 4°C and the PNS removed and maintained on ice prior to loading on gradient within 10 min of removal. Total protein concentration was measured (below). From the supernatant, a 225  $\mu$ l aliquot was subjected to ultracentrifugation for fractionation as described above using either (5%/35%/42.5) sucrose or OptiPrep™ as the gradient. The fractions were stored at  $-80^{\circ}\text{C}$  for a maximum of 6 months.

### Protein assay

The total protein present in each lysate or per fraction was measured by a BCA protein assay (Pierce) using the microplate procedure as directed by the manufacturer. A 10  $\mu$ l aliquot of each fraction was used for the protein assay. Sample absorbance was read at 540 nm. Protein concentrations ranged from 2–3  $\mu\text{g}/\text{ml}$ .

### Cholesterol assay

Fractions were thawed on ice and 50  $\mu$ l of each fraction used to determine the amount of cholesterol according to manufacturer instructions (Cayman Chemicals). Total cholesterol was quantified as a fluorescent resorufin product measured at an emission wavelength of 590 nm using a microplate reader (Molecular Devices, Sunnyvale, CA). The Softmax Pro 4.3LS software was used for data collection (Molecular Devices).

### Western blot analyses

Lysate fractions were thawed on ice. High-density fractions (fractions 14 and 15) were pooled. As protein concentration does

not provide a true baseline parameter for comparison across fractions, equal sample volume loading was used for the Western blot, as previously described (10, 19). This loading method accounts for differential separation of proteins into specific fractions following density ultracentrifugation. From each fraction, an equal sample volume (15  $\mu$ l) was loaded onto 4–12% SDS polyacrylamide gels and run at 125V for 1.5 h. Protein was transferred onto PVDF membranes (Invitrogen) at 30V for 1.5 h. Membranes were incubated with 1:1,000 dilution of an antibody to flotillin 1 (Flot1) to identify the low-density raft fractions. Invitrogen Western Breeze Chemiluminescent kits were used for protein detection and densitometric analysis of identified protein bands was conducted using a Kodak Digital Imaging system Model 440CF (Eastman Kodak, Rochester, NY). Membranes were stripped and reprobed with a 1:500 dilution of an antibody to TfR to identify nonraft fractions. Membranes were additionally probed separately with a 1:500–1:1,000 dilution of the MBP antibody and 1:333 dilution of the GRASP65 antibody. GRASP65 (Golgi reassembly and stacking protein, 65 kDa) is an important structural component required for maintenance of Golgi apparatus integrity and as such serves as a structural marker. For 3-month-old brains, blots probed with MBP were exposed up to 1 h and SuperSignal West Pico Chemiluminescent substrate was used to obtain the brightest possible band.

## RESULTS

To determine which fractions best reflected a “raft-like” nature, we used the following criteria: (1) low protein content, (2) high cholesterol content, (3) Flot1 presence, and TfR absence (48).

### Protein concentration across fractions

Raft fractions have a low protein content: less than 50  $\mu\text{g}$  per fraction (48). In fact, less than 10–30 separate proteins may reside in any given raft compartment at one time (51). Therefore, we measured the protein content of each fraction. Isolation with detergent-free buffer followed by fractionation along a sucrose gradient yielded the lowest protein content in the lightest density fractions 1–5, between 25 to 225  $\mu\text{g}/\text{ml}$  (Fig. 1A). The levels were higher in nonraft fractions. These results suggest that rafts are present within the first 5 low-density fractions. With OptiPrep™ as the gradient, protein levels were lowest in fraction 1 at 100  $\mu\text{g}/\text{ml}$  (Fig. 1B), peaked in fraction 2 ( $\sim$ 500  $\mu\text{g}/\text{ml}$ ) and remained elevated in fractions 3–5. This pattern suggests that with OptiPrep™, only fraction 1 is consistent with raft criteria.

When we compared fractions obtained using our detergent lysis buffer with the sucrose gradient, we found that the detergent method yielded the lowest protein levels in potential DRM fractions 1–3 (Fig. 1C). In contrast, the OptiPrep™ gradient yielded high protein concentrations across the top fractions. This was inconsistent with them being raft fractions (Fig. 1D).

### Cholesterol content across fractions

Fractionation along a sucrose gradient yielded the most consistent distribution pattern for cholesterol content across fractions. Total cholesterol levels were highest in

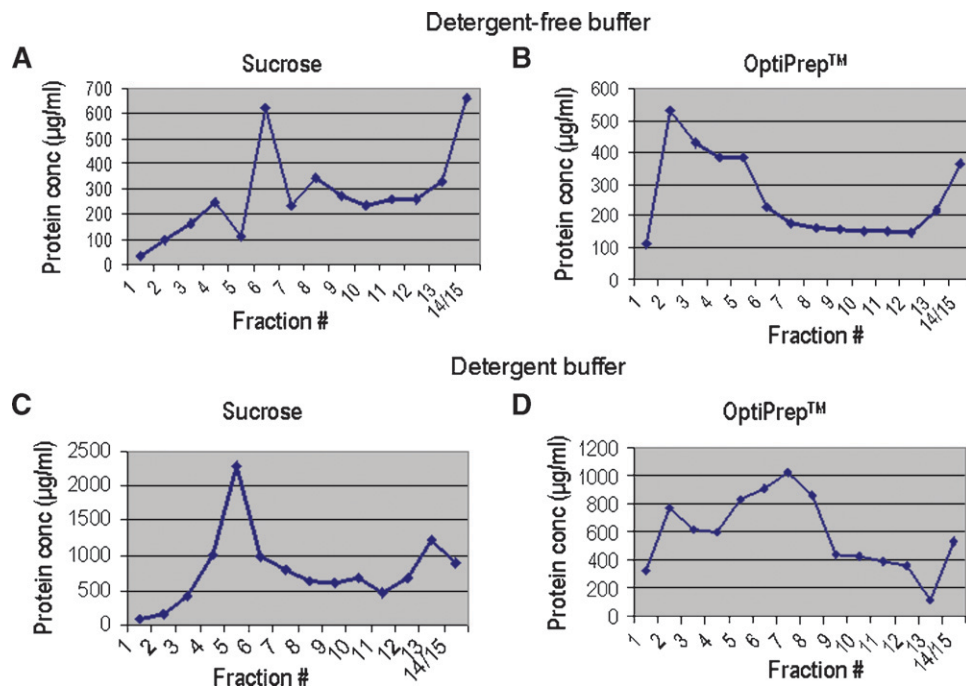


**Fig. 1.** Total protein content in fractions isolated with sucrose and Optiprep™ gradients. A: Total protein content of each fraction following lysis with detergent-free buffer and separation along a sucrose gradient. B: Total protein content of each fraction following lysis with detergent-free buffer and separation along an Optiprep™ gradient. C: Total protein content of each fraction following lysis with 1% Triton-X 100 buffer and separation along a sucrose gradient. D: Total protein content of each fraction following lysis with 1% Triton-X 100 buffer and separation along an Optiprep™ gradient. Values represent total protein in µg/ml.

fractions 1–3 with a peak level of 0.32 µM detected in fraction 3 (Fig. 2A), suggesting that these were raft fractions. With Optiprep™ as the gradient, cholesterol levels in fractions 1–3 were similar to that seen with the sucrose gradient (Fig. 2B); however, a more gradual decline in cholesterol content was observed across fractions 3–9.

We then compared cholesterol levels in fractions obtained using the detergent lysis buffer. We found that both gradient methods yielded different distribution patterns across fractions, compared with that seen with the non-detergent method. In general, the cholesterol levels were high in fractions 2 and 3 with sucrose (Fig. 2C) and fraction 1 with Optiprep™ (Fig. 2D), but fluctuated throughout raft and nonraft fractions.

#### Distribution of Flot1 and TfR across fractions

Next, we examined the distribution pattern across fractions for Flot1, as a marker for raft fractions, and TfR, as a marker for nonraft fractions, after detergent-free isolation. The sucrose density gradient yielded the best resolution of Flot1 in raft fractions (Fig. 3). Dense staining for Flot1 was present in fractions 1–5 with the highest levels in fractions 2–4 (Fig. 3A). In addition, TfR was not detected in fractions 1–3, but was present at peak levels in fractions 6–7 and then declined with increasing fraction density (Fig. 3A). This pattern identifies fractions 1–3 as “true raft” fractions and is consistent with the literature (48). With Optiprep™ as the gradient medium, Flot1 was maximally present in

fractions 1–5, and declined with increasing fraction number (Fig. 3B). TfR was absent from fractions 1–2, highest in fractions 3–5, and declined over the remaining higher density fractions (Fig. 3B). This method suggests that fractions 1 and 2 are the raft fractions.

In comparison to isolation using the detergent lysis buffer, the distribution of marker proteins along the detergent-derived gradient did not clearly indicate raft vs. nonraft fractions. Flot1 was absent from fractions 1 and 2, while present in fractions 3–14/15 (Fig. 4A). The highest intensity occurred in fractions 4–7 representing a 2-fraction shift toward the higher densities, as compared with the nondetergent method. TfR was observed in all fractions (Fig. 4A). Using the Optiprep™ gradient, Flot1 was absent from fraction 1, but present in fractions 2–14/15, with the highest intensity occurring in fractions 3–5 (Fig. 4B). TfR was absent in fractions 1–2, highest in fractions 4–7, and declined over the remaining higher density fractions (Fig. 4B).

#### Methodological controls

**Centrifugation time.** Using the nondetergent method, we examined centrifugation times to determine if a shorter spin time of 4 h would decrease possible diffusion effects through the sucrose gradient and therefore result in better resolution of protein markers. While the distribution of TfR into the mid to lower fractions was similar to that seen with the longer centrifugation period, the distinct resolution

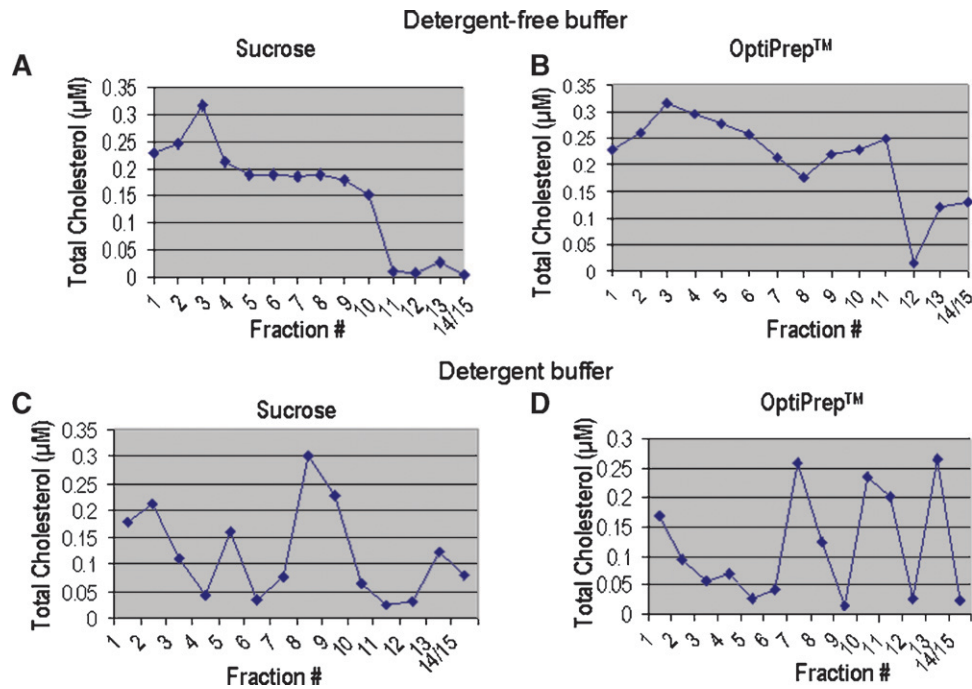


**Fig. 2.** Total cholesterol content in fractions isolated with sucrose and Optiprep™ gradients. A: Total cholesterol content of each fraction following lysis with detergent-free buffer and separation along a sucrose gradient. High cholesterol is present in fractions 1–3, suggesting that these fractions are consistent with raft criteria. B: Total cholesterol content of each fraction following lysis with detergent-free buffer and separation along an Optiprep™ gradient. Cholesterol was high in the low (1–3) and mid-density (4–7) fractions. This suggests that it is difficult to determine which are true raft fractions using this method. C: Total cholesterol content of each fraction following separation along a sucrose gradient with 1% Triton-X 100 as the buffer. High cholesterol in fractions 1 and 2 suggest that these may contain DRMs, but high cholesterol in higher density fractions makes this assertion difficult. D: Total cholesterol content of each fraction following separation along an Optiprep™ gradient with 1% Triton-X 100 as the buffer. High cholesterol in fraction 1 suggests the presence of rafts, but higher cholesterol content of high density fractions, again makes this assertion difficult. Total cholesterol is represented in  $\mu\text{M}$  concentrations.

of Flot1 within fractions was not observed after a 4 h spin time (Fig. 5A).

*Step gradient.* Given the possible confounder that brain tissue is extremely lipid rich, we investigated whether the use of a tighter step gradient might result in better resolution. The raft lysate was subjected to a 5%/20%/30%

sucrose gradient. Under these conditions, the resolution of Flot1 was extremely poor (Fig. 5B). In low-density fractions, Flot1 was not detectable in fractions 1–3, was barely detectable across the midlevel fractions, and was present predominantly in fraction 14/15. Following centrifugation, the liquid was clear with no apparent diffuseness, making it difficult to identify any clear demarcations or

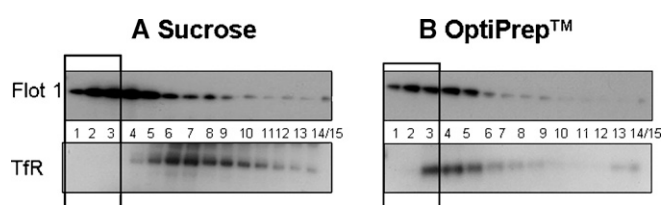


**Fig. 3.** Isolation of rafts with sucrose and Optiprep™ gradients. Top panels show flotillin 1 (Flot1) and bottom panels are transferin receptor (TfR). A: Raft isolation using a detergent-free buffer along a sucrose gradient. Flot1 is maximally present in fractions 1–5. TfR is absent from fractions 1–3. B: Raft isolation using a detergent-free buffer along an Optiprep™ gradient. Flot1 is maximally present in fractions 2–5; TfR is absent from fractions 1 and 2. Blots are representative of three individual experiments. Black bold rectangles designate raft fractions.

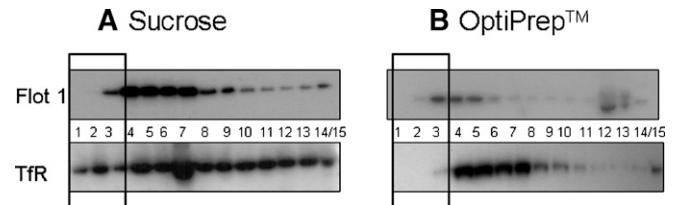


**Fig. 4.** Isolation of detergent resistant membranes (DRMs) with sucrose and Optiprep™ gradients. Top panels show Flot1 and bottom panels are TfR. A: DRM isolation using a 1% Triton-X 100 buffer along a sucrose gradient. Flot1 is maximally present in fractions 3–7. TfR is present in all fractions. B: DRM isolation using a 1% Triton-X 100 buffer along an Optiprep™ gradient. Flot1 is maximally present in fractions 3–5, TfR is absent from fractions 1–3. Black bold rectangles designate DRM fractions. Blots are representative of three individual experiments.

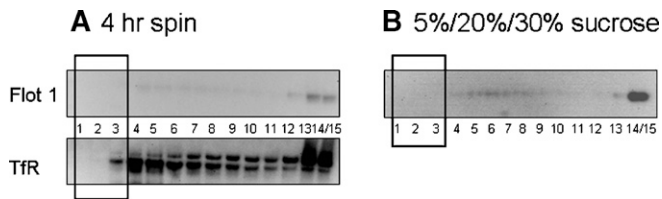


**Fig. 5.** A: Flot1 (top panel) and TfR (bottom panel) distribution following a 4 h centrifugation time. Amount of Flot1 isolated in rafts was less compared with an 18 h spin time. Exposure time for Flot1 was 15 min and 5 min for TfR. B: Distribution of Flot1 following isolation along a 5%/20%/25% sucrose gradient. Isolation and resolution of Flot1 was very poor. Blot shown was exposed for 15 min. Black bold rectangles designate raft fractions.

bands along the gradient. Because the observed Flot1 distribution was indicative of a nonideal preparation of rafts, we did not probe for TfR.

*Myelin contribution.* Myelin content of raft fractions may lead to aberrant shifts by affecting buoyant densities. Therefore, we assessed the integrity of raft fractions further, by testing for the presence of MBP. Two isoforms of mouse MBP were identified, one at 14 kDa and another at 21.5 kDa. The 14 kDa protein was the predominant iso-

form. Since the total amount of MBP in the forebrain accumulates with age, we examined MBP distribution across fractions from PND 21 to 3 months of age using the non-detergent, sucrose gradient method. At PND 21, MBP associates with fraction 3 (**Fig. 6A**). In 3-month-old mice, MBP was evident in fractions 3 and 4 (**Fig. 6B**); however, less than what was seen at the early age. The protein was not detected in any other fraction. PND 21 and 3-month-old animal membranes were exposed for 15 and 30 min, respectively. Additional use of the SuperSignal West Pico chemiluminescent substrate did not enhance the signal further. Together these indicate a very low amount of MBP. As a control we compared the distribution of MBP in the cortex with the brainstem, the latter having higher myelin content (**Fig. 6C**). In both cortex and brainstem, we determined that MBP was present mostly in the pelleted portion of the lysate (**Fig. 6C**). The PNS portion of the lysate contained very little MBP, and, what was present, associated with raft fractions (**Fig. 6C**).

*Golgi association with raft fractions.* As a structural marker for the Golgi apparatus, we examined the distribution of GRASP65 across fractions. In the PND21 mouse cortex, GRASP65 was detected in fractions 3–6 (**Fig. 6A**). In the cortex of 3-month-old mice, GRASP65 could be clearly

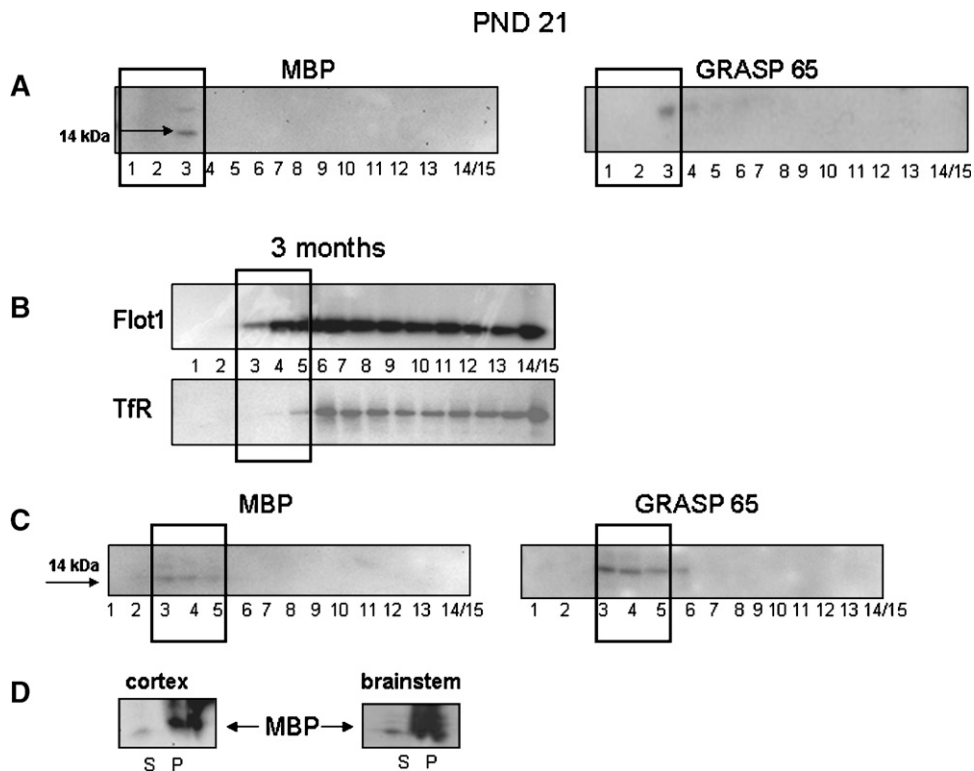


**Fig. 6.** A: Western Blots for myelin basic protein (MBP) and Golgi reassembly and stacking protein 65 (GRASP65) in postnatal day (PND) 21 mouse brain. B: Western blots for Flot1 and TfR in fractions isolated from a 3-month-old C57BL/6 mouse brain. C: Western Blots for MBP and GRASP65 distribution in fractions isolated from a 3-month-old C57BL/6 mouse brain. GRASP65 (46 kDa) was observed in the same raft fractions. D: Western Blots for MBP in the total PNS supernatant versus the pellet isolated from a 3-month-old C57BL/6 mouse brain. Black bold rectangles designate raft fractions. Blots are representative of four individual experiments.

detected in fractions 3–6 (Fig. 6B). At neither age was GRASP65 detected in the lighter fractions, 1–2.

## DISCUSSION

The literature base for raft isolation underscores the highly variable nature of reported procedures. Therefore, a significant level of interest exists in identifying the most accurate isolation technique for each cell or tissue type. Our data add to the growing repertoire supporting the use of detergent-free buffers for rafts preparation and provide a method for isolation of lipid-rich brain tissue. Using the following accepted criteria: 1) low protein content, 2) high cholesterol content, and 3) the presence of Flot1 and absence of TfR, we compared isolated raft fractions in the low-density fractions. Additionally, we looked at the distribution of GRASP65 across the isolated fractions as another control indicator for our protocol. Because we used whole brain tissue, we expected that myelin would be present. Therefore, we also examined the distribution of MBP in the isolated fractions.

Regarding the first criterion, previous work demonstrated that the presence of detergent can influence the partitioning of proteins into rafts and hence can lead to aberrant interpretation of data. Our data were consistent with these reports in that overall higher levels of protein were evident across fractions obtained from a detergent-based isolation, as compared with the nondetergent method. This suggested detergent use could significantly influence data interpretation by affecting the protein distribution across fractions. Direct interference with the BCA protein assay was not expected as this procedure is compatible with up to 5% Triton-X 100. Thus, the nondetergent method provided a cleaner distribution of protein across fractions that met the criteria for identifying raft fractions.

Previous studies utilized sucrose buffers in the isolation of phosphoproteins and lipid rich myelin from brain tissue (26) in order to preserve organelle and membrane integrity. In this study, we compared the use of sucrose versus the commercially available sucrose-based gradient medium, OptiPrep™ that has been used for raft isolation (52). While OptiPrep™ provides an iso-osmotic environment (52) through the addition of sucrose, we found that isolation along a solely sucrose gradient yielded more consistent results. Typically, the fractions pulled off the gradient should range in density from 1.03 g/ml at the top of the gradient, where the raft fractions are present, to 1.165 g/ml at the bottom (39). The use of a sucrose gradient, in combination with the detergent-free buffer, produced a distribution profile of protein content consistent with raft identification with low protein amounts in the low-density, upper 3 fractions. When this feature was examined with an OptiPrep™ gradient, it resulted in high protein concentrations in upper fractions, a condition that is not consistent with these fractions being low density or representative of rafts. This sucrose gradient pattern more closely matched that generated in cultured cells by Macdonald and Pike (48), and supports it as the choice of


gradient for raft isolation from brain tissue. In addition to the protein distribution, an inverse pattern was demonstrated for cholesterol content. Consistent with the Macdonald and Pike (48) method, cholesterol content was higher in the low-density fractions. This pattern was not as clear with the OptiPrep™ gradient and was highly variable when a detergent-lysis buffer was used.

Other studies on isolated cells or subcellular fractions have used buffers containing EDTA (47, 53), which may prevent the proper isolation of rafts (48). We have eliminated EDTA from our detergent-free buffer, but have added sodium fluoride and sodium orthovanadate to inhibit serine/threonine and tyrosine protein phosphatase activity. We have kept cations as they can have a stabilizing effect on rafts, even allowing their isolation at 37°C (18). In previous efforts to optimize isolation procedures for rafts, Song et al. (46) subjected sonicated cells to a 16–20 h ultracentrifugation spin through a discontinuous 5%/35%/45% sucrose gradient. However, sonication may result in excessive protein recovery (48) and long centrifugation times may lead significant contamination with other membranes. The method we employed for brain tissue required a short preparation time followed by an 18 h ultracentrifugation step at 38,500 rpm (200,000 *g*). Despite this lengthy spin step, our data demonstrate that with mouse brain, the better resolution of marker proteins (e.g., Flot1) along the gradient occurs with an 18 h spin, compared with a 4 h one. Regarding to the length of the procedure, the rapid preparation of the sample makes the 18 h overnight centrifugation step somewhat optimal for scheduling and completion of the assay.

In addition to the ultracentrifugation times, we also examined separation along a slightly different sucrose gradient. We tried a tighter 5%/20%/30% gradient in an attempt to cater for the large amount of lipid-rich myelin. However, this gradient did not prove to be optimal for resolution of raft-associated proteins from brain tissue, as evidenced by the absence of Flot1 in the low-density fractions. By comparison, the 5%/35%/42.5% sucrose gradient provided good resolution of Flot1 in the top fractions and TfR in the heavier fractions from brain tissue.

As additional characterization of our protocol, we examined the distribution of MBP within raft fractions. Our data indicate that MBP in PND21 animals is restricted to only one of the raft fractions, fraction 3. To determine if this was a technical anomaly or an age-related effect, we examined tissue from 3-month-old mice and demonstrated that MBP appears to be distributed at lower levels over 3 fractions (3, 4, and 5). This redistribution in myelin may be due to increased deposition and/or appearance of heavier myelin that occurs as a function of age (40). Thus, the small amount of MBP present in the PNS from the cortex remains distributed across the raft fractions. This limited MBP distribution across the fractions suggests that there is minimal contamination from other lipid membranes. Although our data demonstrated that MBP-associated rafts can be isolated from whole brain tissue using this protocol, it is clear that most of the myelin has been eliminated from the PNS and was retained within the pellet. This is sup-

ported by previous studies (41, 54) and indicates that clean raft fractions with little myelin contamination in the PNS can be prepared with our protocol. Here we demonstrate a distinction between the DRMs of isolated myelin, where all raft-associated fractions contained MBP, and rafts isolated from whole brain tissue by our detergent-free protocol. In DRMs isolated from bovine myelin, sucrose density gradient separation showed an enrichment of MBP in fractions 4–6; in myelin from mice between 2 and 8 months of age, MBP was observed in the DRM fractions (41). Interestingly, we observed that there seems to be an age-related developmental shift in Flot1 distribution that occurs around 3 months of age in the mouse. This shift results in fractions 3, 4, and 5 becoming the raft fractions instead of 1–3. This shift does not appear to be due to the changes in myelin or MBP distribution, as PND 21 mice show MBP presence in fraction 3. The age factor should therefore be taken into consideration when choosing tissue sources for raft isolation. Further discussion of this point is beyond the scope of this paper.

To further characterize our protocol, we examined the distribution of GRASP65. Golgi fragmentation has been linked to neurodegenerative pathways, and GRASP65 can serve as an indicator of cellular disruption (32, 55). GRASP65 was associated with raft fraction 3 and the heavier fractions 4 and 5 at both PND21 and 3 months of age. There are no previous studies that document GRASP65 association with rafts; however, our results are in agreement with reports documenting association of other Golgi markers with rafts (48, 56). The consistent distribution of GRASP65 in raft and slightly heavier nonraft fractions at both ages indicates that our method of lysis and fractionation worked well. The use of our protocol can, therefore, reproducibly produce fractions that are highly representative of rafts (i.e., presence of Flot1 and absence of TfR, high cholesterol and low protein) from unprocessed, fresh or frozen, brain tissue. 

Thank you to Drs Alex Merrick and Xiao-Ping Yang for their critical reading of this manuscript and helpful suggestions.

## REFERENCES

- Brown, D. A., and E. London. 2000. Structure and function of sphingolipid- and cholesterol-rich membrane rafts. *J. Biol. Chem.* **275**: 17221–17224.
- Simons, K., and E. Ikonen. 1997. Functional rafts in cell membranes. *Nature*. **387**: 569–572.
- Simons, K., and R. Ehehalt. 2002. Cholesterol, lipid rafts, and disease. *J. Clin. Invest.* **110**: 597–603.
- Lagerholm, B. C., G. E. Weinreb, K. Jacobson, and N. L. Thompson. 2005. Detecting microdomains in intact cell membranes. *Annu. Rev. Phys. Chem.* **56**: 309–336.
- Dietrich, C., B. Yang, T. Fujiwara, A. Kusumi, and K. Jacobso. 2002. Relationship of lipid rafts to transient confinement zones detected by single particle tracking. *Biophys. J.* **82**: 274–284.
- Edidin, M. 2003. The state of lipid rafts: from model membranes to cells. *Annu. Rev. Biophys. Biomol. Struct.* **32**: 257–283.
- Kay, J. G., R. Z. Murry, J. K. Pagan, and J. L. Stow. 2006. Cytokine secretion via cholesterol-rich lipid raft-associated SNAREs at the phagocytic cup. *J. Biol. Chem.* **281**: 11949–11954.
- Kim, H. Y., S. J. Park, E. H. Joe, and I. Jou. 2006. Raft-mediated Src homology 2 domain-containing protein tyrosine phosphatase 2 (SHP-2) regulation in microglia. *J. Biol. Chem.* **281**: 11872–11878.
- Fullekrug, J., and K. Simons. 2004. Lipid rafts and apical membrane traffic. *Ann. N. Y. Acad. Sci.* **1014**: 164–169.
- Persaud-Sawin, D. A., L. Banach, and G. J. Harry. 2008. Raft aggregation with specific receptor recruitment is required for microglial phagocytosis of A $\beta$ 42. *Glia*. In press.
- Chichili, G. R., and W. Rodgers. 2007. Clustering of membrane raft proteins by the actin cytoskeleton. *J. Biol. Chem.* **282**: 36682–36691.
- Davis, A. R., G. Lotocki, A. E. Marcillo, W. D. Dietrich, and R. W. Keane. 2007. FasL, Fas, and death-inducing signaling complex (DISC) proteins are recruited to membrane rafts after spinal cord injury. *J. Neurotrauma*. **24**: 823–834.
- Shimizu, K., M. Okada, K. Nagai, and Y. Fukada. 2003. Suprachiasmatic nucleus circadian oscillatory protein, a novel binding partner of K-Ras in the membrane rafts, negatively regulates MAPK pathway. *J. Biol. Chem.* **278**: 14920–14925.
- Ford, T., J. Graham, and D. Rickwood. 1994. Iodixanol: a nonionic isosmotic centrifugation medium for the formation of self-generated gradients. *Anal. Biochem.* **220**: 360–366.
- Lingwood, D., and K. Simons. 2007. Detergent resistance as a tool in membrane research. *Nat. Protoc.* **2**: 2159–2165.
- London, E., and D. A. Brown. 2000. Insolubility of lipids in triton X-100: physical origin and relationship to sphingolipid/cholesterol membrane domains (rafts). *Biochim. Biophys. Acta.* **1508**: 182–195.
- Lichtenberg, D., F. M. Goni, and H. Heerklottz. 2005. Detergent-resistant membranes should not be identified with membrane rafts. *Trends Biochem. Sci.* **30**: 430–436.
- Chen, X., A. Jen, A. Warley, M. J. Lawrence, P. J. Quinn, and R. J. Morris. 2008. Isolation at physiological temperature of detergent-resistant membranes with properties expected of lipid rafts: the influence of buffer composition. *Biochem. J.* **417**: 525–533.
- Arvanitis, D. N., W. Min, Y. Gong, Y. M. Heng, and J. M. Boggs. 2005. Two types of detergent-insoluble, glycosphingolipid/cholesterol-rich membrane domains from isolated myelin. *J. Neurochem.* **94**: 1696–1710.
- Heffer-Laue, M., G. Laue, L. Nimrichter, S. E. Fromholt, and R. L. Schnaar. 2005. Membrane redistribution of gangliosides and glycosylphosphatidylinositol-anchored proteins in brain tissue sections under conditions of lipid raft isolation. *Biochim. Biophys. Acta.* **1686**: 200–208.
- Heffer-Laue, M., B. Viljetic, K. Vajn, R. L. Schnaar, and G. Laue. 2007. Effects of detergents on the redistribution of gangliosides and GPI-anchored proteins in brain tissue sections. *J. Histochem. Cytochem.* **55**: 805–812.
- Radeva, G., and F. J. Sharom. 2004. Isolation and characterization of lipid rafts with different properties from RBL-2H3 (rat basophilic leukaemia) cells. *Biochem. J.* **380**: 219–230.
- Chen, X., R. Morris, M. J. Lawrence, and P. J. Quinn. 2007. The isolation and structure of membrane lipid rafts from rat brain. *Biochimie.* **89**: 192–196.
- Won, J. S., Y. B. Im, M. Khan, M. Contreras, A. K. Singh, and I. Singh. 2008. Lovastatin inhibits amyloid precursor protein (APP) beta-cleavage through reduction of APP distribution in Lubrol WX extractable low density lipid rafts. *J. Neurochem.* **105**: 1536–1549.
- Hancock, J. F. 2006. Lipid rafts: contentious only from simplistic standpoints. *Nat. Rev. Mol. Cell Biol.* **7**: 456–462.
- Suneja, S. K., Z. Mo, and S. J. Potashner. 2006. Phospho-CREB and other phospho-proteins: improved recovery from brain tissue. *J. Neurosci. Methods.* **150**: 238–241.
- Yu, W., K. Zou, J. S. Gong, M. Ko, K. Yanagisawa, and M. Michikawa. 2005. Oligomerization of amyloid beta-protein occurs during the isolation of lipid rafts. *J. Neurosci. Res.* **80**: 114–119.
- Brown, D. A., and J. K. Rose. 1992. Sorting of GPI-anchored proteins to glycolipid-enriched membrane subdomains during transport to the apical cell surface. *Cell.* **68**: 533–544.
- Schuck, S., M. Honsho, K. Ekroos, A. Shevchenko, and K. Simons. 2003. Resistance of cell membranes to different detergents. *Proc. Natl. Acad. Sci. USA.* **100**: 5795–5800.
- Ehehalt, R., P. Keller, C. Haass, C. Thiele, and K. Simons. 2003. Amyloidogenic processing of the Alzheimer beta-amyloid precursor protein depends on lipid rafts. *J. Cell Biol.* **160**: 113–123.
- Fantini, J., N. Garmy, R. Mahfoud, and N. Yahi. 2002. Lipid rafts: structure, function and role in HIV, Alzheimers and prion diseases. *Expert Rev. Mol. Med.* **4**: 1–22.
- Persaud-Sawin, D. A., J. O. McNamara 2nd, S. Rylova, A. Vandongen, and R. M. Boustany. 2004. A galactosylceramide binding domain is involved in trafficking of CLN3 from Golgi to rafts via recycling endosomes. *Pediatr. Res.* **56**: 449–463.



33. Tashiro, Y., T. Yamazaki, Y. Shimada, Y. Ohno-Iwashita, and K. Okamoto. 2004. Axon-dominant localization of cell-surface cholesterol in cultured hippocampal neurons and its disappearance in Niemann-Pick type C model cells. *Eur. J. Neurosci.* **20**: 2015–2021.
34. Hinman, J. D., C. D. Chen, S. Y. Oh, W. Hollander, and C. R. Abraham. 2008. Age-dependent accumulation of ubiquitinated 2',3'-cyclic nucleotide 3'-phosphodiesterase in myelin lipid rafts. *Glia.* **56**: 118–133.
35. Harder, T., and K. Simons. 1997. Caveolae, DIGs, and the dynamics of sphingolipid-cholesterol microdomains. *Curr. Opin. Cell Biol.* **9**: 534–542.
36. Simons, K., and J. Gruenberg. 2000. Jamming the endosomal system: lipid rafts and lysosomal storage diseases. *Trends Cell Biol.* **10**: 459–462.
37. Simons, K., and D. Toomre. 2000. Lipid rafts and signal transduction. *Nat. Rev. Mol. Cell Biol.* **1**: 31–39.
38. Igbavboa, U., G. P. Eckert, T. M. Malo, A. E. Studniski, L. N. Johnson, N. Yamamoto, M. Kobayashi, S. C. Fujitani, T. R. Appel, W. E. Müller, et al. 2005. Murine synaptosomal lipid raft protein and lipid composition are altered by expression of human apoE 3 and 4 and by increasing age. *J. Neurol. Sci.* **229–230**: 225–232.
39. McCaffrey, G., et al. 2007. Tight junctions contain oligomeric protein assembly critical for maintaining blood-brain barrier integrity in vivo. *J. Neurochem.* **103**: 2540–2555.
40. Siegel, G. J. 1998. Molecular, cellular and medical aspects. In *Basic Neurochemistry*, 6th edition. Lippincott-Raven, Philadelphia. 86–90.
41. DeBruin, L. S., J. D. Haines, D. Bienzle, and G. Harauz. 2006. Partitioning of myelin basic protein into membrane microdomains in a spontaneously demyelinating mouse model for multiple sclerosis. *Biochem. Cell Biol.* **84**: 993–1005.
42. Lappe-Siefke, C., S. Goebbels, M. Gravel, E. Nicksch, J. Lee, P. E. Braun, I. R. Griffiths, and K. A. Nave. 2003. Disruption of Cnp1 uncouples oligodendroglial functions in axonal support and myelination. *Nat. Genet.* **33**: 366–374.
43. Simons, M., E. M. Krämer, C. Thiele, W. Stoffel, and J. Trotter. 2000. Assembly of myelin by association of proteolipid protein with cholesterol- and galactosylceramide-rich membrane domains. *J. Cell Biol.* **151**: 143–154.
44. Molander-Melin, M., K. Blennow, N. Bogdanovic, B. Dellheden, J. E. Månsson, and P. Fredman. 2005. Structural membrane alterations in Alzheimer brains found to be associated with regional disease development; increased density of gangliosides GM1 and GM2 and loss of cholesterol in detergent-resistant membrane domains. *J. Neurochem.* **92**: 171–182.
45. Eckert, G. P., U. Igbavboa, W. E. Müller, and W. G. Wood. 2003. Lipid rafts of purified mouse brain synaptosomes prepared with or without detergent reveal different lipid and protein domains. *Brain Res.* **962**: 144–150.
46. Song, K. S., Li Shengwen, T. Okamoto, L. A. Quilliam, M. Sargiacomo, and M. P. Lisanti. 1996. Co-purification and direct interaction of Ras with caveolin, an integral membrane protein of caveolae microdomains. Detergent-free purification of caveolae microdomains. *J. Biol. Chem.* **271**: 9690–9697.
47. Smart, E. J., Y. S. Ying, C. Mineo, and R. G. Anderson. 1995. A detergent-free method for purifying caveolae membrane from tissue culture cells. *Proc. Natl. Acad. Sci. USA.* **92**: 10104–10108.
48. Macdonald, J. L., and L. J. Pike. 2005. A simplified method for the preparation of detergent-free lipid rafts. *J. Lipid Res.* **46**: 1061–1067.
49. Shah, M. B., and P. B. Sehgal. 2007. Nondetergent isolation of rafts. *Methods Mol. Biol.* **398**: 21–28.
50. Liu, J., P. Oh, T. Horner, R. A. Rogers, and J. E. Schnitzer. 1997. Organized endothelial cell surface signal transduction in caveolae distinct from glycosylphosphatidylinositol-anchored protein microdomains. *J. Biol. Chem.* **272**: 7211–7222.
51. Yoshizaki, F., H. Nakayama, C. Iwahara, K. Takamori, H. Ogawa, and K. Iwabuchi. 2008. Role of glycosphingolipid-enriched microdomains in innate immunity: microdomain-dependent phagocytic cell functions. *Biochim. Biophys. Acta.* **1780**: 383–392.
52. Li, X., and M. Donowitz. 2008. Fractionation of subcellular membrane vesicles of epithelial and nonepithelial cells by OptiPrep density gradient ultracentrifugation. *Methods Mol. Biol.* **440**: 97–110.
53. Kelly, J. F., K. Storie, C. Skamra, J. Bienas, T. Beck, and D. A. Bennett. 2005. Relationship between Alzheimer's disease clinical stage and Gq/11 in subcellular fractions of frontal cortex. *J. Neural Transm.* **112**: 1049–1056.
54. DeBruin, L. S., J. D. Haines, L. A. Wellhauser, G. Radeva, V. Schonmann, D. Bienzle, and G. Harauz. 2005. Developmental partitioning of myelin basic protein into membrane microdomains. *J. Neurosci. Res.* **80**: 211–225.
55. Nakagomi, S., M. J. Barsoum, E. Bossy-Wetzel, C. Sütterlin, V. Malhotra, and S. A. Lipton. 2008. A Golgi fragmentation pathway in neurodegeneration. *Neurobiol. Dis.* **29**: 221–231.
56. Nichols, B. J., A. K. Kenworthy, R. S. Polishchuk, R. Lodge, T. H. Roberts, K. Hirschberg, R. D. Phair, and J. Lippincott-Schwartz. 2001. Rapid cycling of lipid raft markers between the cell surface and Golgi complex. *J. Cell Biol.* **153**: 529–541.